

CONTROL OF KARST CAVES SAFETY IN THE POŁOM LIMESTONE QUARRY

Zbigniew BEDNARCZYK*, Maria BRYCH*,
Sławomir PATLA*

Institute of Opencast Mining, Poltegor-Institute, Parkowa 25, 51-616 Wrocław, Poland

Abstract: The purpose of the study was to monitor the impact of mining on the structure of crystalline limestone caves, in the vicinity of a quarry in SW Poland. The scope of work included an analysis of the geological and geotechnical conditions and safety of the caves. The research included the application of MASW Multichannel Analysis of Surfaces Waves to determine rock voids, identification of geotechnical parameters and slope stability. Short-range aerial photogrammetry was used to produce maps. Seismometers and glass plates installed near and inside the caves allowed characterization of V^s parseismic vibration velocity, acceleration, displacement and frequency. The MASW survey determined V_s velocity and limestone strength. The 48-m long survey revealed several zones with higher values of V_s and cave zone with lower values of 70–90 m/s. It allows the identification of the cave. The slope stability analysis, taking into account the results of the geophysical survey, previous research and field observations, indicates that the slope is stable. In the second part, the magnitude of vibrations was measured as a function of charge size and distance. The research was conducted to determine the parameters of safe blasting operations, detect the caves using MASW method and minimize negative impact of exploitation on the caves. A methodology for monitoring the condition of rock slopes in the vicinity of blasting sites was presented. In the conclusions, the geotechnical parameters and the stability of the quarry slope near the caves were characterized. It was found that the slopes are stable with factor of safety $F_{os} > 10$. Investigations confirmed that using MASW method it is possible to detect caves and strength parameters up the depth of over 20 m. It was also possible to determine the safe level of parseismic vibration of $v = 2.45$ cm/s for the studied caves.

Keywords: *quarries, control of vibrations, geotechnical engineering, geophysics, slope stability analysis*

*Corresponding authors: zbigniew.bednarczyk@igo.wroc.pl (Z. Bednarczyk), maria.m.brych@gmail.com (M. Brych), slawomir.patla@prokopa.pl (S. Patla).

1. INTRODUCTION

Limestone opencast mining is carried out on a large and small scale in many countries worldwide for the manufacturing of cement and lime. This type of mining can have several implications for the environment, changes in landscape, instability of rock masses, and other effects. Blasting can result in the damage to slopes in surrounding areas, the dislodging of large blocs from rock walls and it also could pose a threat to karsts cave ecosystem formed over millions of years. The use of explosives could also damage groundwater circulation. Falling rocks can also be dangerous that need to be controlled. Some of the caves require permanent, strict protection (Kasprzyk et al. 2015; Kurpiewski 2018; Szykiewicz 2012; Sobczyk et al. 2016; Bin, Zhengyu et al. 2016). The lack of sufficient knowledge about the caves concerns both institutions and individuals responsible for environmental protection and services appointed to realize this task. Another problem is connected with the classification of these unique natural sites. Environmental protected objects are classified either as areas of occurrence of specific protected animal or plant species or inanimate nature areas. The caves sometimes escape these criteria, especially in mining areas, so it is important to devise effective methods for its monitoring and protection (Bin, Zhengyu et al. 2016; Kurpiewski 2018). Caves constitute a unique environment of fauna and flora that do not occur outside them and were formed over millions of years. They are also places of the underground water circulation network accessible to man. As a result, they are the most susceptible to anthropogenic pollution. Caves in the vicinity of mines are frequently not accessible to the public and often are not subject to special care. This underscores the pressings and necessity important to devise effective methods for its monitoring, protection and systematic monitoring. This knowledge should be incorporated into mining management and exploitation plans. Caverns may also result in the unintentional accumulation of pumped explosives, leading to the excessive scattering of rock fragments outside the designated flyrock zone. It may also pose a threat to people and machinery through the formation of a sinkhole (Kotyrbá 2018). The most effective mitigation method is the utilization of non-invasive exploration technologies, which will enable the identification of caves and rock voids before the commencement of mining operations. Furthermore, the necessity of rational extraction of the deposit, namely the utilization of available, discovered, and documented resources in such a manner that the total extraction is achieved simultaneously with the protection of valuable sites, necessitates the undertaking of research and additional documentation. Different seismic and resistivity geophysical methods or geological drilling could be applied to gain a comprehensive interpretation of cavities and karst caves occurrence (Bin, Zhengyu et al. 2016; Bullen 1963; Santamarina 1994; Sanchez-Salineró et al. 1987; Sheu et al. 1988). However, the precise recognition of slope parameters in quarries necessitates the implementation of

costly drilling operations and strength laboratory tests. Same types of geophysical investigations could be not fully sensitive for cave location (Szynkiewicz 2012; Sobczyk et al. 2016; Kasprzak et al. 2019). Consequently, to reduce the costs, it is important to try to adopt new geophysical methods of scanning to check its possibilities to locate rock voids existing in the deposit. This together with careful monitoring could help in protection of the caves.

The investigations presented were conducted near the caves located in SW Poland in of Połom Hill near the Wojcieszów. The limestone from examined quarry is extracted for the production of aggregate and limestone meal on seven levels in a slope-deep excavation. In the mine's close vicinity, thirteen caves are located (eight protected). Bajda, Górecki 1996; Bochynek 2016; Dziedzic, Gruszecki 1992; <https://jaskiniepolski.pgi.gov.pl/Details/Information/3986>. A distinctive feature of the investigated quarry is the formation of rock voids that, from the perspective of mining operations, are a technological and geotechnical threat to the safety of the exploitation. The investigations objective was to incorporate different geotechnical, geophysical and mining monitoring methods to recognize the cave location, strength parameters, slope stability and influence of blasting mining method on the cave safety. These included interpretation of geotechnical parameters of the slope above the caves based on previous investigations, new implementation of MASW shallow geophysical scanning method for detection of existing and not discovered caves, measurements of paraseismic vibrations, short-range aerial photogrammetry for actualization of quarry morphology, field observations and slope stability analysis for prediction of quarry wall stability. These methods allowed detection of the caves in the cross-sections, characterization of the geotechnical stability parameters, actualization of the morphology and recognition safe for the caves paraseismic vibration levels. In the conclusions, results from the performed investigation were discussed and the safe values of vibration levels in the caves were defined.

2. LOCALIZATION AND GEOLOGY OF THE DEPOSIT

The "Połom" crystalline limestone deposit is situated in the Lower Silesia voivodship (Figs. 1 and 2). It is located approximately 1 km west of the main road passing through the city, on the left bank of the Kaczawa River, above Upper Wojcieszów. The deposit is situated within the Kaczawskie Mts., which form part of the Western Sudetes Mts. and run from NW to SE. The complex tectonic structure was formed in many polygenetic stages. The crystalline limestones were formed from carbonate rocks and metamorphosed. They were altered in zones of epi- and meso-metamorphism. These older rocks are cut by veins of younger porphyry (rhyolite). The boundaries of the geological units are mostly tectonic, marked by zones of faults and overthrusts, foliated and

crossed by faults and quartz veins. Limestones form an inclined fold with monoclinal dips. Folding and subsequent movement have created a dense network of multidirectional fractures, small folds and faults with variable dip. Metamorphic rocks such as greenschist and greenschist shales, phyllites, sericite shales, quartz shales, crystalline limestones, porphyroids are of Upper Cambrian age. The following rock complexes were identified in the area: the Radzimowice shale, the Wojcieszow limestone, the Greenschist shale, the Diabasic shale and the Phyllite series (Bajda, Górecki 1996; Dziedzic, Gruszecki, 1992). The Połom Hill Quarry is situated at an altitude of 667 metres a.s.l. The coordinates of the quarry bottom are 530 metres above sea level. The relative heights of the surrounding area do not exceed 300 m. Karst processes are expressed by the presence of fractures, cavities, caves and funnels, often filled with clay and rock debris. The fissures and cavities are conducive to the rapid infiltration of rainwater. Active quarries surround the top of Połom on two sides. The overburden has been removed over the entire surface of the deposit.

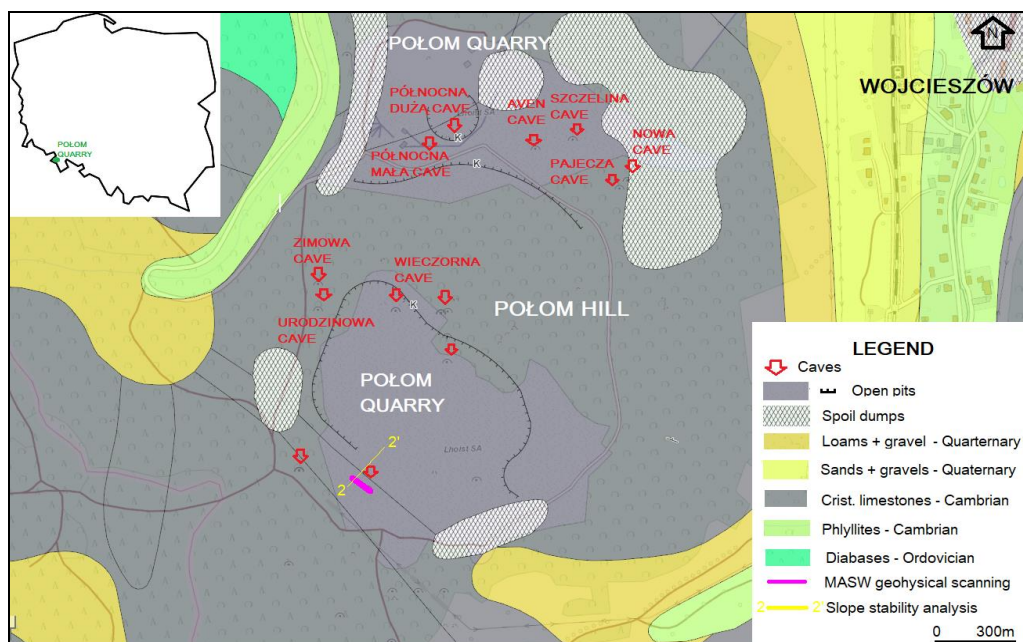


Fig. 1. Location and geological map of the studied area
(on the basis of Detailed geological map of Poland 1:50 000, 2011)

The main type of rock is used in the lime industry as hydrated lime or for fertilising and deacidifying soils. Aggregates and lime meal are used in road construction. Limestone has also been used as a decorative stone. No groundwater has been identi-

fied in the deposit to be exploited.

3. CHARACTERISTICS OF PROTECTED CAVES

The caves can be described as fissure caves in the limestone beds, which were formed by the development of underground karst processes. The caves may have a rich and varied speleothems brown and red calcite coatings, draperies, cascades, ribs, organs, stalactites. The most attractive are the rhombohedral crystals formed in the conditions of stagnant thermal water. The caves location in the immediate vicinity the Połom Hill, is shown in Figs. 2 and 3 in relation to the current and planned extent of mining (Żuk et al. 2011). The protected caves are located: a) about 330 m to the north of the mine – Północna Duża, Północna Mała, Ostrych Kantów, Wojcieszowska Gap, Aven Cave, b) about 350 m to the north-east: Pajęcza Cave and Nowa Cave, c) about 540 m to the north-west: Lejowa Cave, Nad Potokiem Cave, d) Urodzinowa Cave and Zimowa Cave. A general view of the mine, the mining area boundary, and the current and projected extent of mining with explosives influence in relation to the location of protected caves are shown in Fig 2. The Północna Duża Cave was discovered in 1924. The cave is 103 m long, 39 m deep and the height of the opening is 587 m a.s.l. Behind the opening there is a large main hall, 45 m long, 20–25 m wide and 4–5 m high. The cave contains many stalactites and has a microclimate similar to that of a “static ice cave” with the permanently low temperature. Bats spend the winter in the cave. The Północna Mała Cave has a total length of 23.4 m. The cave has the character of a washed out limestone stream bed. The cave has the shape of a collapsed mine shaft. Wojcieszowska Rift Cave has been known since the 1950s, i.e. since the opening of the quarry. It is 440 m long and 112.6 m deep. The cave is described as the deepest in Poland after the Tatra Mountains caves with bats and spiders. Its bottom is 93 m below the entrance. The cave is 108 m long and 27 m deep. It is 1.1 m wide and 1.2 m high. The Pajęcza Cave has a low entrance. Behind it there is a big chamber – a room measuring 4.6 m × 8.6 m. The cave is named after a rather numerous, 60 m long, population of cave webworms, spiders of the species *Meta Menardi*. The entrance to the Nowa Cave has a short corridor leading to a large room. In this hall, in a small hollow under the E wall, a small lake appears periodically. The cave is very wet. Bats can be found in the large hall. There are also troglloxenes, bees, spiders and moths in the chimney and at the opening. The Zimowa and Urodzinowa caves are the closest to the present site and are protected. Discovered in 2000/2001, the caves with entrance created by mining on the west slope of the mine. These caves are regularly monitored by the speleological team due to the presence of bats. Inside the Zimowa Cave, a fissure meter has been installed. The cave has been chosen to measure vibrations from mining operations in the vicinity of blasting (Fig. 3). Since 2000, the number of bats

in the cave has been regularly monitored by the staff of the Zoological Institute of the University of Wrocław in cooperation with the Wrocław University of Life Sciences, the Wrocław Chiropterological Group, the Czech Speleological Society Liberec and the Grotołazy Wrocław. Nocturnal listening for social and echolocation calls was also conducted in summer 2011 (Żuk et al. 2011). In total, about 300–400 bats of 11 species are observed hibernating every winter (Kurpiewski 2018).

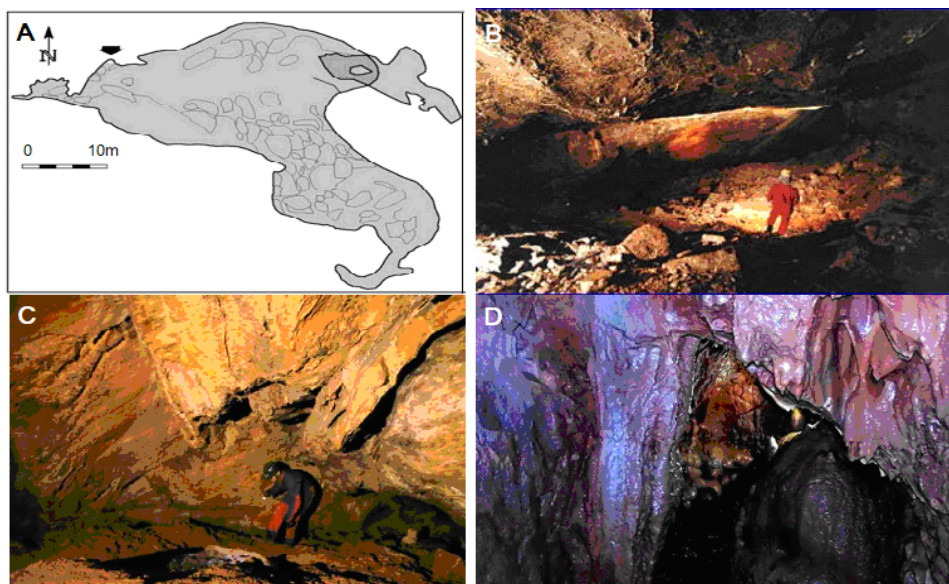


Fig. 2. The Północna Duża Cave: A – map of the cave, B – lower hall, C – upper hall, D – stalagmites

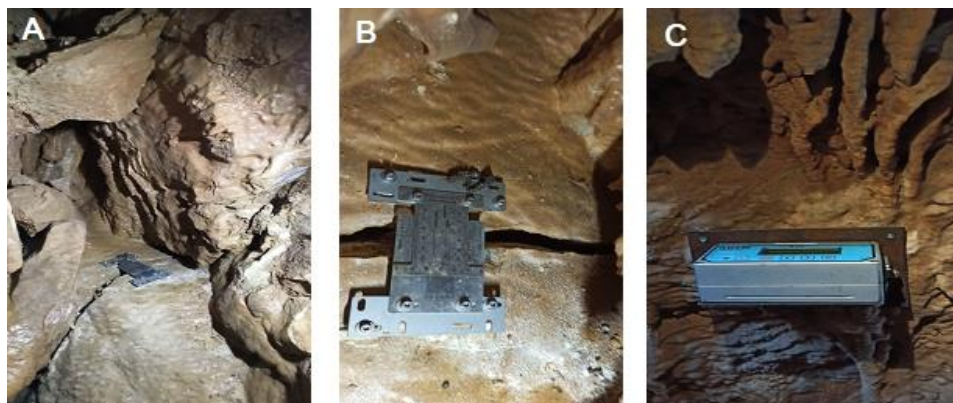


Fig. 3. The Zimowa Cave with installed monitoring devices: A, B – feeler gauges, C – Vibralock

4. GEOLOGICAL ENGINEERING CONDITIONS

The exploitation of the Połom deposit, which lasted for several hundred years, resulted in a significant transformation of the entire massif, which is tectonically complex and highly fractured. Taking into account the complex geological and mining conditions, it is classified in the 3rd group of deposit variability. The massif has a varied tectonic and folded structure. On the tectonic foundations, crevices, caverns (caves) and karst funnels filled with clay and rock debris have been formed. The deposit is bordered on the east by the valley of the Kaczawa River. Infiltration of rainwater into the massif is facilitated by (generally open) cracks and fissures in the rock mass, a high degree of karstisation and the presence of cracks and caves, especially on the western slope of the quarry. During heavy rainfall, rainwater can accumulate at the bottom of the quarry, but the ability to drain water from the open pit means that there has been no groundwater hazard to mining operations. Initially, the slopes were 1–12 m high, with an inclination of 60–70° and a shelf width of about 9 m. After 2000, these were changed to 20 m high and 5–6 m wide. The geological structure of the area near the performed investigations is shown on cross-section in Fig. 4. It is characterised by SW and NE dipping tectonic faults. The layers of light-coloured limestones of the lower horizon are separated by layers of phyllites, phyllitic shales and calcareous phyllites, which dip at an angle of about 45° to the NE. The strength of the rocks showed that the limestone has a strength 82–174 MPa and a bulk density = 2.7 g/cm³ (Bajda, Górecki 1996). However, these results may be overestimated as they do not take into account fracturing and karstification. The porosity of the limestones ranges from 1.43 to 6.23%, the water absorption from 0.1 to 0.4%. Selected strength parameters characterising the quarried limestones are summarised in Table 1.

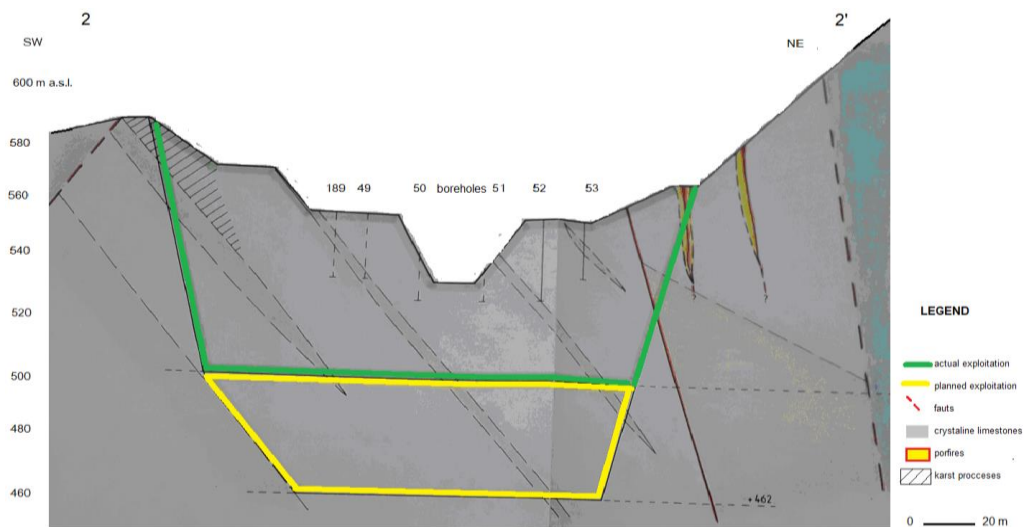


Fig. 4. Geological cross-section 2-2' scale 1:1000 (location in Fig. 1)

Table 1. Selected quality parameters of crystalline limestones from the Polom deposit

Parameter	Value (mean value)
Uniaxial compression R_c [MPa]	82–174 (116)
Density [g/cm ³]	2.76–2.89 (2.81)
Apparent density [g/cm ³]	2.68–2.75 (2.71)
Porosity [%]	1.43–6.23 (3.62)
Soakability [%]	0.1–0.4 (0.2)
Frost resistance (cycles)	25 (cycles)
Frost resistance (% weight loss)	0.0–0.8 (0.4)
CaCO ₃ content [%]	85.5–97.83 (92.83)

5. METHODS

The methods chosen for the investigation including non-invasive MASW geophysical scanning, paraseismic vibration monitoring, UAV photogrammetry and numerical slope stability analyses. These methods allows detection and prediction of safety, stability of quarry slopes and protected natural and speleological sites and also delivered new data and the addition of geological documentation for subsequent parts of the deposit. Therefore, with a view to optimum extraction and the safety of mining operations, the

possibility of adapting the microseismic apparatus to locate rock voids existing in the deposit was examined. Obtained data allowed also actualization of the quarry morphology and prediction of safe for the caves paraseismic vibrations levels.

The MASW (Multichannel Analysis of Surface Waves) is a non-invasive geophysical method for investigating soils and rocks. It has been used in engineering geophysics since the 1990s. The primary objective of MASW measurements is to accurately estimate the elastic properties of soils and rocks, their approximate geological structure and geomechanical parameters. The MASW method makes it possible to identify the propagation of surface seismic waves on the basis of parameters such as wave speed and attenuation. Surface waves propagate to different depths depending on their frequency. This makes it possible to determine the elastic properties of soils and rocks (Bullen 1963; Nazarian et al. 1983; Park et al. 1997; Santamarina 1994). The dispersion of surface waves depends on the physical characteristics of the substrate, mainly on their variations in the vertical profile. By determining the scattering curves, the strength characteristics of the soil or rock can be determined. This method is characterised by the possibility of continuously recording very small deformations or voids. This offers the possibility of a more accurate identification of the elastic properties of the soil or rock under investigation. It is based on the measurement of the velocity of surface seismic waves, during impact with a hammer or by means of another seismic vibration generator (Fig. 5). Seismic waves generated at the surface of the soil or rock, propagate both as longitudinal and transverse waves that propagate throughout the rock mass and Rayleigh surface waves near the ground surface. In the MASW method, a multi-channel seismograph is connected to a string of geophones that record surface wave propagation velocities. MASW analyses low-frequency waves from 2 to about 30 Hz, made possible by purpose-built geophones. Due to the relatively high accuracy of the method, which is achieved through both measurement and data processing techniques, this enables information on the structure and strength characteristics of the rock mass to be obtained quickly. MASW allows not only a quantitative representation of the elastic properties of the subsoil in the form of a shear wave profile V_s , but also a qualitative representation of the picture of near-surface heterogeneity and heterogeneity of the bedrock.

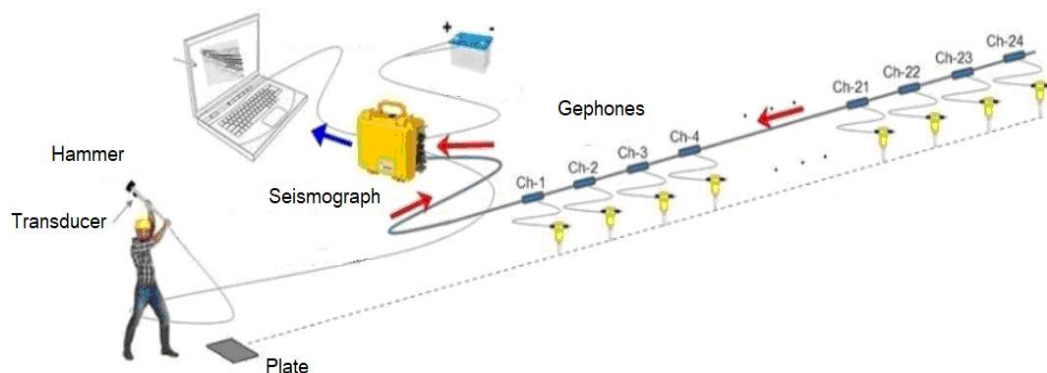


Fig. 5. Method of performing the MASW test using a multi-channel (24 geophones) recording system (Park et al. 1997)

The UAV photogrammetry was used to observe the condition of the rock face was the use of an unmanned aerial vehicle and the post-evaluation of pre- and post-blasting photographs of the rock face taken with a 1" CMOS / 20 megapixel camera and an 84° 8.8 mm / 24 mm lens.

The paraseismic vibration measurements are relay on ground velocity, acceleration, displacement and frequency recording in the moment of blasting. Seismometer measures the wave parameters in one vertical and two horizontal directions, in line: quarry – object. Measured values of seismic effect presented in function of distance and size of fired explosives, taking into consideration geological and mining propagation of vibrations conditions. On this basis the mathematical model of seismic vibrations radiation was specified. In in order to preserve the homogeneous structure of limestone caves is necessary to know the safe level of paraseismic vibrations generated by mining. In previous works (Žuk 2011; Kurpiewski 2018) the calculation of safe charges in this mine was carried out with the assumption of the permissible vibration magnitude for protected caves as $V_d = 0.25$ cm/s. In comparison, in the German standard DIN 4150, in buildings it should not exceed $V_d = 0.5$ cm/s and for sensitive buildings $V_d = 0.3$ cm/s.

A comparison with the Polish standard is not possible, as the results of the measuring device must be analyzed in 1/3-octave bands before their magnitude can be assessed on the scale of dynamic influences (on buildings). The safe vibration level for the protected objects has a real impact on the range of blasting operations.

The slope stability analyses was carried in one cross-section located on the west slope the quarry near the investigated cave area out using Flac 7.0 software and the Shear Strength Reduction Method (SSR). A linear elastic constitutive soil model was used for the calculations. The SSR method aims to reflect the real processes leading to the reduction of the shear strength of the rock or soil forming the slope until it loses its stability. The slope stability factor Fos was calculated using the finite difference

method. Analyses of the rock mass boundary condition, took into account the expected depth of the groundwater level, allowed the values of the parameters in certain nodes of the model to be estimated. These values were approximated by Lagrange interpolation method and presented in isolinear form as shear strain rate [s^{-1}] or maximum velocity vector [m/s]. It allowed prediction of the slope stability in investigated area.

6. RESULTS OF GEOPHYSICAL MICROSEISMIC SURVEYS (MASW)

The MASW surveys were carried out on the SW slope at 578 m a.s.l., in a 50 m section (Figs. 5–9). The region is characterised by the presence of intensive karst phenomena between 580–540 m a.s.l. Their thickness increases significantly towards the SE from about 10 m in section 1-1', to 20 m in section 2-2', to a maximum of 40 m in section 3-3'. The MASW method, allows the V_s profile to be obtained in the 1-D profiles and in 2-D cross sections. The measurements from 24 geophones with a frequency of 4.5 Hz, spaced every 2 m were recorded by a high quality multichannel seismograph. The investigations were carried out in the following stages: a) collection of archive maps and engineering geological data, b) field work – setting up the geophysical equipment along the surveyed section, installation of geophones, connection and testing of the equipment, c) calibration of the seismograph, input of measurement data, definition of the measurement method, checking of noise and correct operation of the seismograph, d) data acquisition, a total of 26 measurements, e) analysis and interpretation by the “stacking method” with extraction of the dispersion curve for each measurement. In this method, a multi-channel recording of the measurement data was decomposed into individual frequency components of the seismic waves using the Fast Fourier Transform (Bullen 1963). Amplitude normalisation was then applied to each frequency. The number of phase shifts required to determine the time delay for each frequency component. Finally, they were all added together to give the summed energy for the different frequency components of the wave (Park et al. 1997). The interpretation included: a) back-inversion analysis to determine the shear wave velocity V_s as a function of depth, b) construction of a preliminary shear wave velocity model, c) construction of V_s 1D profile models for individual geophones – 24 profiles in total (Fig. 6) construction of 2D MASW cross-sections by interpolating the MASW V_s 1D cross-sections (Fig. 7). The survey made it possible to determine in detail the values of the V_s shear wave velocity to a depth of 8 m in the twelve 1D profiles. Their example is shown in Fig. 5. It shows in detail the seismic wave velocities down to a depth of 18 m. The darker dark grey colour indicates the bedrock layers with large variations in V_s velocity.

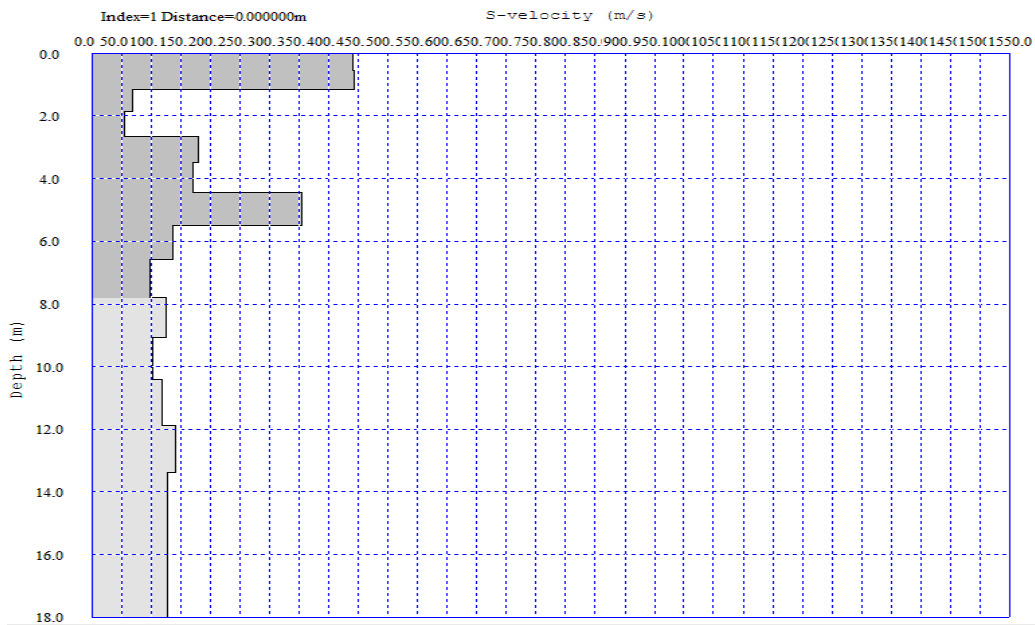


Fig. 6. Example of a 1D seismic wave velocity profile at 4 and 40 m from geophone 1

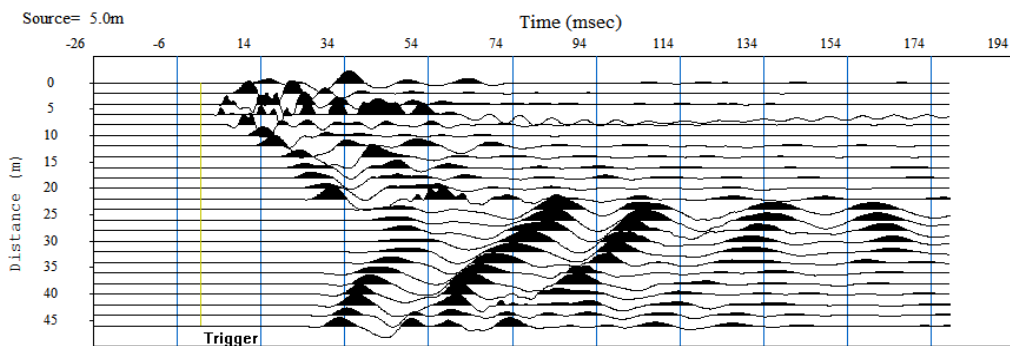


Fig. 7. MASW 2D Measurement, seismic wave triggered +5 m from geophone No. 1

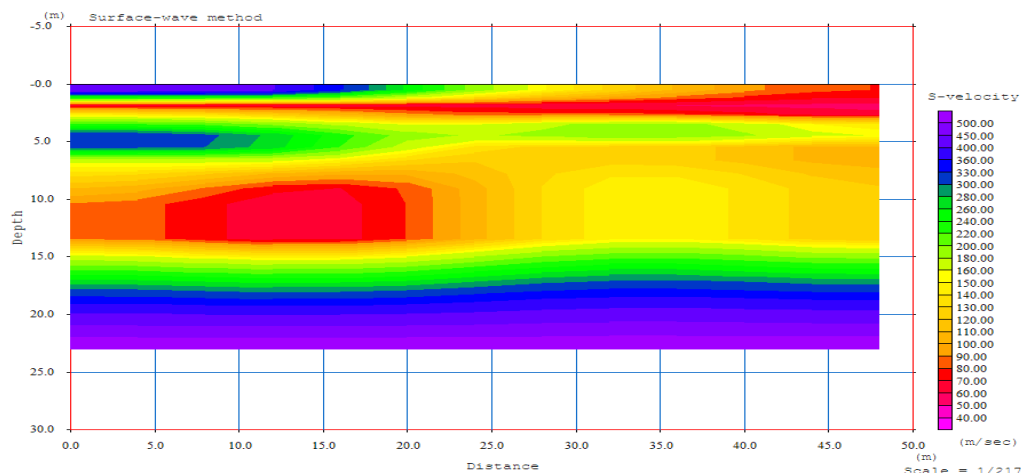


Fig. 8. MASW results – 2-D section of shear wave velocity V_s [m/s]

The interpretation of all the measurements taken is shown in Fig. 8. It shows several zones with significantly higher shear wave velocity values of 360–500 m/s (in blue) and an isolated oval zone (cave?) with lower V_s values of 70–90 m/s (in red). The highest variability of velocity occurring in the first 22 metres of the surveyed section, where the above oval zone with significantly lower V_s values occurs. It is located at a depth of 8–14 m in the area where the geological documentation of the deposit recorded the occurrence of intensive karst phenomena between depths of 580–540 m a.s.l. It is about 10 m in cross-section 1-1' to 20 m in cross-section 2-2'. These results indicate the possibility of detecting karst phenomena in MASW geophysical surveys. Areas of markedly different shear wave velocities are also evident in the twelve 1D V_s (s velocity m/s) profiles at distances from 0 m to 44 m, every 4 m. These show that the greatest differences along the length occur in the first 16 m of the profiles taken. It was found that there are the zones characterised by different shear wave velocities V_s (Table 4). Up to a depth of about 8 m there is a very large variation in shear wave velocity from 50 to 450 m/s. Two depth intervals with high wave velocities 0–1 m and 4.5–5.5 m and two intervals 4.5–5.5 m and 7–8 m with lower velocities are clearly visible. There is less variation in shear wave velocity in the further 1D profiles representing 16–44 m of profiling. Analysis of the 2D shear wave velocities allowed rock characterisation to a depth of 22.5 m.

The interpretation of the MASW 2D cross-sections allowed interpretation of N -coefficient values (Fig. 9). However, these values cannot be used directly for stiff rocks, but could contain important data related to their mechanical characteristic (these values represent strength parameters in SPT soundings in soils and fractured rocks). Interpretation of the MASW results showed that the strength parameters of rock

mass are highly variable. The N -factor values ranged from $N = 2$ to $N = 48$ (Table 3). These values, when compared with those presented in Table 2, indicate that the rock mass can range from loose (voids, fractures) to very compact, the angle of internal friction can range from 28 to 41° and the bulk density is $1600\text{--}2100\text{ kg/cm}^3$. However, this interpretation is based on general relationships and in future should be refined by correlations based on local conditions and representative number of laboratory strength tests.

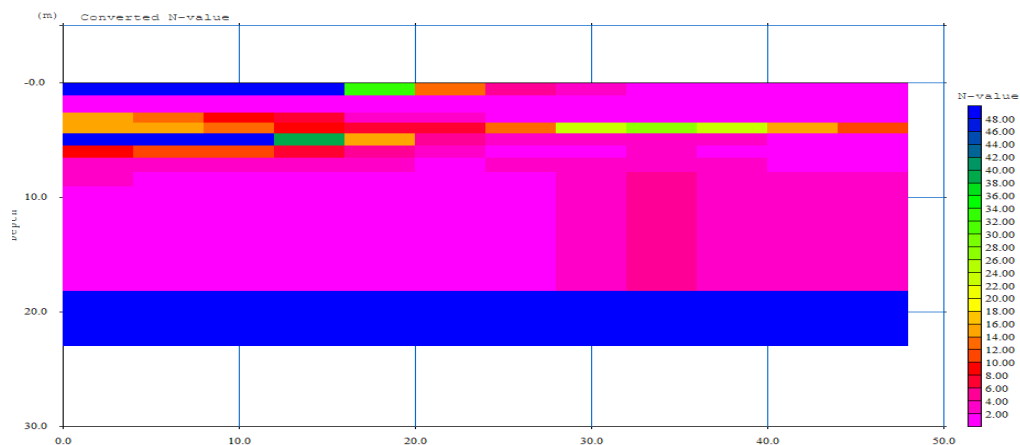


Fig. 9. MASW results – 2D section of N -values, representing strength parameters in SPT

Table 2. Summary of the zones with a high level of V_s variability

No.	Location on the cross-section [m]	Depth [m]
1	0	7.9
2	4	7.9
3	8	6.5
4	12	7.9
5	16	7.9
6	20	2.7
7	24	2.2
8	28	2.6
9	32	2.2
10	36	2.5
11	40	2.5
12	44	2.6

Table 3. Interpretation of the N -values (correlation of the soil strength MASW/SPT)

No.	Depth [m]	Location on the cross-section [m]	N -value
1	0.0–1.0	0–20; 20–48	34–48; 4–12
2	1.0–2.0	2.0–6.0	4–48
3	2.0–3.0	0–20; 27–48	12–18; 26
4	5.0–6.0	0–20; 20–48	10, 6
5	6.0–17.5	0–48	2–6
6	17.5–22.0	0–48	48

Table 4. Velocities of the seismic shear wave V_s at the quarry level to a depth of 22.5 m

Depth [m]	Location on the cross-section [m]	V_s [m/s]	Remarks
0.00–1.25	0.0–20.0	300–400	green colour in Fig. 8
0.00–2.00; 1.25–2.00	17.5–27.0; 0.0–17.5	200–280	green colour in Fig. 8
0.00–2.50; 1.25–2.5	27.0–48.0; 0.0–27.0	90–160	orange colour in Fig. 8
4.00–6.00	0.0–8.0	330–400	blue colour in Fig. 8
7.00–2.50	0.0–20.0	160–180	green colour on Fig. 8
7.50–13.00	0.0–22.5	70–90	red colour in Fig. 8 karst, cave ?

7. RESULTS OF SLOPE STABILITY ANALYSIS

The slope stability analysis was carried out near the site of the geophysical survey. The cross section 2-2' (Figs. 4, 8, 9 location in Fig. 1) was selected along the line of maximum slope inclination. Parameters of limestone uniaxial compressive strength and bulk density from the geological documentation were used. For other rock types, comparable parameters from other studies were included (Table 5). The GSI classifications enabled to interpret the rock strength parameters (Hoek, Brown 1980). This classification allowed to analyse stresses that lead to loss of stability of slope using the correlation between model parameters and the GSI strength index. The basis of the Hoek–Brown criterion was to compare the strength of intact rock and add factors that reduce it. This classification takes into account a number of factors such as the degree of rock fracturing, mining method, location within the slope, rock type and uniaxial compressive strength. Relationship between stress state and rock evaluation was performed according to the RMR classification (Bieniewski 1989). Based on the GSI classification, the parameters of the massif were determined according to the following formulae:

$$m_b = m_i e^{(GSI-100/28-14D)}, \quad (1)$$

$$s = e^{(GSI-100)/9-3D}, \quad (2)$$

$$a = \frac{1}{2} + \frac{1}{6}(e^{(-GSI/15)} - e^{(-20/3)}), \quad (3)$$

where:

GSI – Geological Strength Index,

D – coefficient of failure of the rock mass,

m_i – material strength constant of intact rock.

Table 5. Design parameters used in the calculations

No.	Layer	Type of rock	R_c [MPa]	ρ [kN/m ³]	c [MPa]	φ [°]
1	I	Crystalline limestone (light)	82.0	2.76	2.24	18.36
2	II	Phyllites	50.0	2.52	1.14	15.02
3	III	Karst formations limestone residuals	3.0	2.20	1.12	9.18
4	IV	Karst limestone residuals cave voids	1.00	2.00	0.23	6.26

For numerical modelling of slope stability, four geological-engineering layers with different strength parameters were separated. The geometry of the layers is shown in Fig. 10. The algorithm of the Flac software required the declaration of the volume density, porosity, effective cohesion values and angle of internal friction of the rocks and the depth of occurrence of groundwater. A summary of strength parameters are given in Table 5. This made it possible to the zones of greatest deformation within the slope. In the calculations performed, horizontal displacements were blocked at the right and left edges, allowing only free movement in the vertical direction. On the other hand, vertical displacements were blocked at the lower edge, allowing movement in the horizontal direction. The slope surface was a free surface. The introduced grid density had dimensions of 1×1 m. The results of the calculations carried out are shown in Fig. 11. The analyses showed high slope stability factor $F_{os} = 10.49$. The slope is stable (it is assumed when $F_{os} > 1.5$). The analysis detected that the highest shear stresses will occur near the area of the karst caves at the height of 540–550 m a.s.l. in the central part of the analysed section. It should also be emphasised that the analysis of slope stability may not be fully representative due to the lack of strength laboratory tests and more than 25 years since the documentary studies. Geotechnical conditions may have changed since that time. Errors could related to uncertainty of strength and geometric parameters (Wiłun 2010). The introduced parameters are approximate and based on archive drillings and the so-called comparable experience.

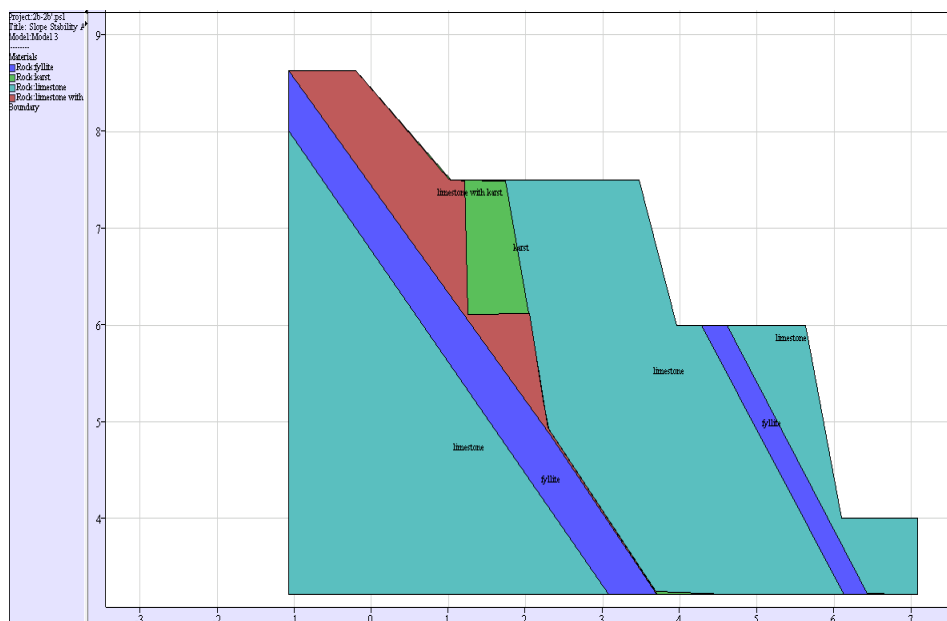
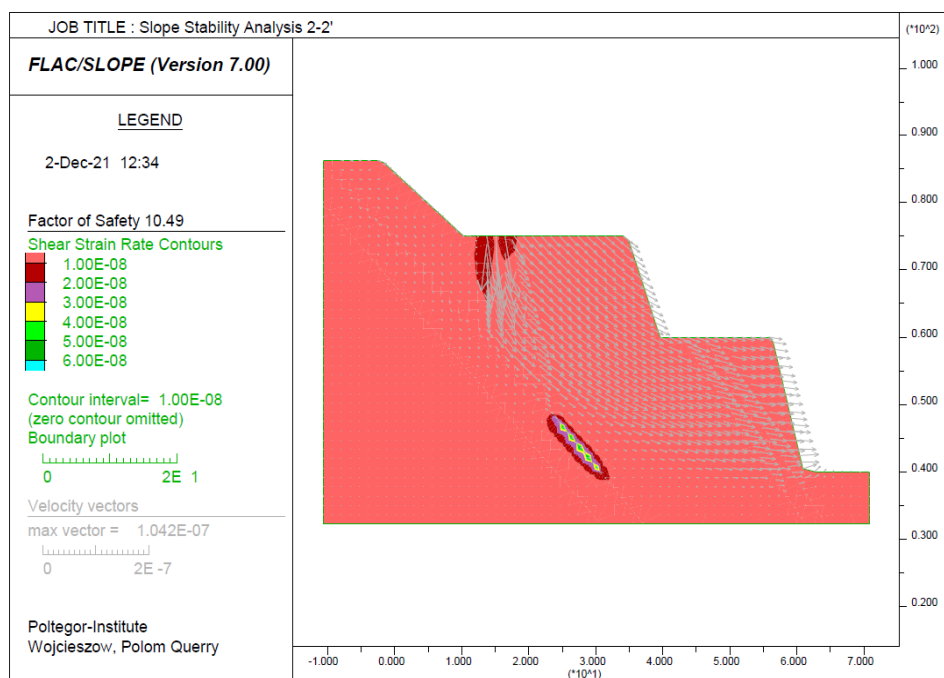


Fig. 10. Slope stability analysis, model of layers geometry model

Fig. 11. Slope stability analysis, shear stresses, factor of safety $F_{os} = 10.49$

8. RESULTS OF PHOTOGRAMMETRY

Short-range aerial photogrammetry was used to minimise the impact of blasting operations and to provide accurate terrain mapping. A GPS receiver located characteristic points of known coordinates in the field. From a height of about 50 m above the ground, the unmanned aircraft took successive series of photographs. With a specific size of the on-board digital camera matrix, flight speed and altitude, the measurement accuracy was about 1.5 cm per pixel. At the end of the mission, the data were downloaded to a personal computer and, using specialist computer software, were subjected to time-consuming processing based on the measured terrain points to produce a high-precision numerical terrain model. The second stage of minimizing the impact of blasting was based on the design of the blast grid on the digital model obtained. The mapping carried out made it possible to select the geometry of the blast grid on the basis of the amount of blasting over the entire height and length of the face, as well as the volume of the blast. It was possible to select the amount of explosive, the diameter of the hole, localization of stemming and the choice of delay time to ensure the desired fragmentation and seismic effect. The designed boreholes were plotted on the terrain model and appropriate drilling angles were set. The third stage involved the implementation of the design assumptions in the field. Continuous control of drilling parameters was implemented.

9. RESULTS OF PARASEISMIC VIBRATION MONITORING

The aim of the study was to determine the safe level of paraseismic vibrations generated by mining in order to preserve the homogeneous structure of limestone caves. At the Połom mine, mining is carried out with explosives using the method of long and short vertical blastholes at six levels. Exploitation in the areas where blasting mining is not permitted should be mechanical, using mining machinery such as a skidder or hydraulic hammer. If the charges and blasting parameters are proper, it will result in correct fragmentation, lack of oversize, ergonomic shape of the repository, and at the same time the safety. Due to the lack of mining fronts in the immediate vicinity of accessible, rock cavities, where it would be possible to install a sensor to measure vibrations and observe possible changes in the condition of quarry walls, the study was carried out in accessible, safe locations. The locations of the blasts and the measurement points are shown in Fig. 12. In total, the following parameters were recorded: displacement amplitude, velocity, acceleration and vibration frequency. The results are summarized in Table 6. The values of the wave and the observation of changes in the structure of the protected object were compared. The following parameters were analyzed: vibration velocity, acceleration, displacement and frequency. Due to the

considerable distance of the caves from the actual blast front, the observations were made at the level of the rock face adjacent to the blast. In order to observe the impact of the paraseismic wave on the rock face, glass plates were attached to selected fractures in the rock face using construction plaster. Four monitoring points were established for blast II, III and IV. Two points were in the immediate vicinity of the blasted area. In order to measure the vibrations acting on the cave wall and the rib of the excavation, the instrumentation was installed on specially adapted steel plates, fixed with 8 cm long anchors. The apparatus for measuring vibrations was also placed on the wall of the Winter Cave, due to the safety and security regulations (Fig. 3). During blast II located at a distance of $d = 39$ m from the nearest blast borehole, the maximum vibration level was $v = 2.45$ cm/s. No changes were observed in the glass plates. During blasts III and IV on apparatus, located at a distance of $d = 21$ m from the nearest blast borehole, the maximum vibration level was $v = 6.99$ cm/s and $v = 2.02$ cm/s, respectively.

Table 6. Parameters of test blasting works

No.	Parameter		Unit	Blast I Sept. 30	Blast II Oct. 6	Blast III Oct. 11	Blast IV Oct. 11	Blast V Nov. 9	Blast VI Nov. 9
1	Bench height	H	m	15	21	20	20	21	8
2	Blasthole depth	L	m	16	22	20.7	20.3-20.5	22	9
3	Sub-drill	p	m	1	1	0.5	0.5	1	1
4	Stemming height	l_p	m	3	3	3	3-3.5	3	3
5	Burden	z	m	3	3	3.2	3	3	3
6	Blastholes spacing	a	m	3.2	3.2	3	3.2	3.2	3
7	Row spacing	b	m	3	3	3	3	3	2.7
8	Number of boreholes to be fired	n	No	36	30	30	30	27	98
9	Number of rows	I	No	3	3	3	2	3	8
10	Hole diameter	φ	mm	105	105	105	105	105	105
11	Blasthole inclination	α	degree	80	80	80	80	80	85
12	Maximum charge per delay	Q_z	kg	110.8	129.7	130	126.5	145	35.95
13	Total charge	Q_c	kg	3238	3890	3890	3785	3912.1	3224.1
14	Level	–	–	3	5	5	6	5	6
15	Floor coordinate	–	m	472	501	501	521	501	520

One of the monitoring points was eliminated by moving rock masses. At another point, cracks in the building plaster and detachment of the glass plate were observed. From the study it is clear that the vibration level of $v = 2.45$ cm/s does not affect the

structure of the rock face, the vibration level of $v = 6.99$ cm/s causes displacement of the rock. To observe the condition of the rock face in relation to the level of vibration magnitude during the IV and V blasting, there were taken the photos before and after the blasting. Control points were marked on the cliff face to allow precise overlay of pre- and post-shot images. In order to protect the instrument, sensor was mounted on the rock face at a distance of $d = 43$ m from the blast. After superimposing the pre- and post-imaging, three test sections located in the immediate vicinity of the control points, were delineated on the photograph and visually assessed for structural changes. The largest vibration magnitudes were recorded at a distance of $d = 21$ m, the maximum vibration velocity on the measuring apparatus was $v = 6.99$ cm/s, with a maximum displacement on the vertical axis of $p = 0.24$ mm.

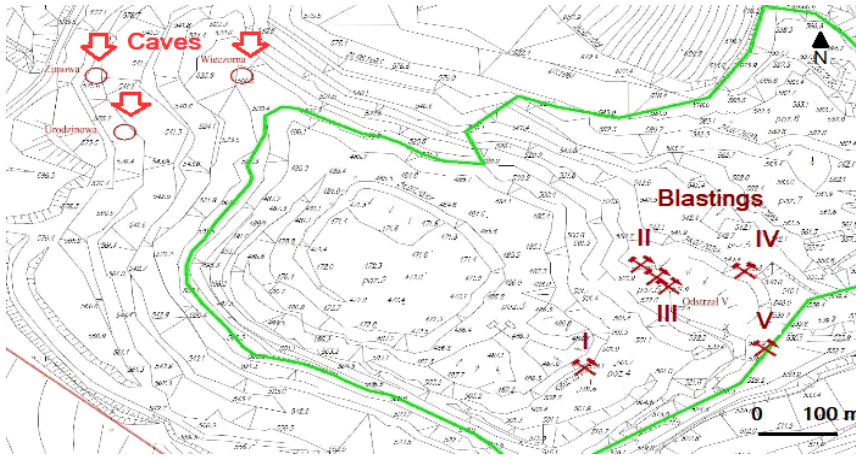


Fig. 12. Location of blasting in relation to delay nearest caves

The model of the vibration propagation was used for determining the magnitude of the blasts that are permitted. Due to the fact that the propagations are characteristic for individual rocks, directions of the parseismic wave, depending on geology, tectonics, rock cavities, cracks and their sizes. The model is not fixed and may change with the progress of mining fronts. Therefore it was determined each time on the basis of in-situ measurements. The initial characterizing the propagation of a wave in a given part of the rock mass are the records of the magnitudes of the vibrations recorded by the measuring devices installed on specially adapted steel plates, fixed with anchors. The results obtained from the instrumentation were related to the parameters of the blasting carried out according to:

$$v = a\rho^b, \quad (4)$$

where:

- v – maximal wave velocity in point [cm/s],
- a, b – coefficients of seismic propagation,
- ρ – reduced charge calculated using Eq. (5).

The coefficients a and b , especially for a rock with a heterogeneous geological structure or characterized by the presence of overgrowth, cavities, are variable. They are related to the geological, factors of the rocks and depend on the mining charges that are not included in the formula, the actual excavation or drilling and the inclination of the blast boreholes. In the case of the research carried out, due to the spatial orientation of the excavation, the fronts currently exploited and the direction of the nearest protected caves, only the profile with a NW–SE course was studied. The reduced charge is determined by a formula that relates the basic measurement parameters, i.e., the distance of the measurement point from the vibration source and the amount of charge applied during the blasting per millisecond delay according to the formula:

$$\rho = \frac{Q_z^n}{d} \text{ [kg}^n\text{/m]}, \quad (5)$$

where:

- Q_z – maximum charge per one degree of millisecond delay,
- d – the distance between the charge firing point and the given measurement point,
- n – power factor depending on mining and geology (according to Žuk 2011; Kurpiewski 2018 as $n = 0.5$).

The combination of relations (4) and (5) gives a mathematical picture of the propagation of vibrations in a given rock on a given measurement profile, taking into account the actual geological-mining conditions and the actual blasting conditions (coefficients a and b , ρ). The superposition of the calculation points took into account the measured vibration magnitudes on the rock face (V_{\max} on the y -axis) and the reduced charge (ρ on the x -axis). Thus, taking into account the reservoir and geological-mining conditions, it was found that the prediction of the vibration velocity depending on the magnitude of the applied charge on the millisecond delay Q_z at the measuring point located at a distance d can be made on the basis of the relationship:

$$V = 22.347 \rho^{1.3842} \text{ [cm/s]}, \quad (6)$$

where ρ is determined by Eq. (5), with the power factor assumed as $n = 0$.

It is possible to predict the magnitude of the vibrations at a distance d from the blasting site as a function of the charge size per millisecond delay used. To determine the charge size per millisecond delay Q_z as a function of the distance of the blasting operation from the protected object a certain limiting of vibration velocity could be assumed (Fig. 13). Using the readings from the measuring apparatus anchored in the rock medium, a mathematical model of the magnitude of the displacements depending

on the value of the reduced charge specified by the formula (5) was determined. Thus, based on the study, the value of displacement can be predicted according to the equation:

$$p = 0,7727 \rho^{1.0107} \text{ [mm]}, \quad (7)$$

where ρ is determined by Eq. (5), with the power factor $n = 0.5$.

The determined equations and the possible magnitude of vibrations could be important for the safe blasting operations for the protection of caves, as well as for the optimal mining of the deposit. However, it should be borne in mind that during progress of exploitation the model of wave propagation may change, so it is worth to verify it repeating the studies.

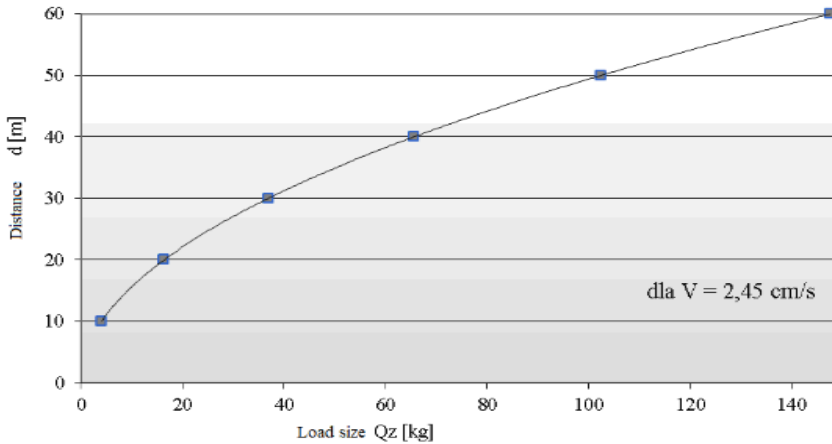


Fig. 13. Charge size diagram for millisecond delay nearest caves as a function. of distance

10. CONCLUSIONS

The geophysical investigations allowed to make a preliminary characterization of the geological and engineering structure of the studied area. An attempt was made to detect rock voids in the “Polom” crystalline limestone deposit by means of a non-invasive MASW method. The measurements were carried out on the SW slope of the mine, at 578 m a.s.l., over a distance of 48 m. It allowed to characterize the strength properties of the rock substrate at the investigated level with different values of shear wave velocity down to a depth of 22.5 m. The survey revealed several zones of shear wave velocity and the existence of an isolated oval zone, which may indicate a cavity or cave. The zones of V_s velocity are highly variable, with the greatest changes occur-

ring in the first 22 meters of the section, where a zone of significantly lower V_s velocity values occurs. These method is seem to be suitable for detection of the caves from the surface of quarry exploitation levels. The usage of Ramac GPR 250 MHz antenna for detection of similar crystalline limestone cave in Śnieżnik Massif in Sudety Mts. was not fully successful (Szynkiewicz 2015). Better geophysical recognition of the karst cave could be obtained by GPR and ERT scanning (Kasprzyk et al 2019). MASW method has its limitation connected with relatively long time of measurements and limited distance but besides the detection of the caves and void it allowed also for the strength parameters characterization. The performed investigations included also slope stability analysis. They took into account the results of the geophysical surveys and indicated that the slope was stable $F_{os} = 10.49$. The determination of more representative rock parameters on the basis on representative number of strength tests, current drilling, mapping and their correlation with additional MASW surveys in other areas of the quarry may provide additional information on rock strength parameters and their spatial distribution. It was determined that the optimal method of monitoring the seismic wave propagation and the stability of the rock faces is a combination of the method of mounting monitoring points with building gypsum and comparative photographic documentation, while using the apparatus for monitoring the magnitude of paraseismic vibrations on the rock face. On the basis of the measurements, a mathematical model for the propagation of paraseismic vibrations was established. These allowed to found the correlation between the vibration velocity and displacement at a distance d from the blasting site as a function of the size of the charge applied per millisecond delay. It was predicted that the velocity of vibrations at the level of $v = 2.45$ cm/s does not violate the structure of the rock face, which, given the same rock medium, can be accepted as a first approximation of the safe level of vibrations for the protection of caves. Due to the unique character of the caves its safety need to be regularly monitored.

ACKNOWLEDGEMENTS

Authors would like to acknowledge Połom Quarry for making the investigation site available. The research was financed by statutory funds of the Poltegor-Institute.

REFERENCES

- BAJDA R., GÓRECKI J., 1996, Appendix No. 1 to the geological documentation in cat. C1 of the Połom crystalline limestone deposit in Wojcieszów, AGH Kraków, Arch. Przedsiębiorstwo Geologiczne Dolnośląskiego Urz. Woj. w Jeleniej Górze.
- BIENIAWSKI Z.T., 1989, *Engineering rock mass classifications: a complete manual for engineers and geologists in mining, civil, and petroleum engineering*, Wiley-Interscience, 40–47.
- BIN L., ZHENG YU L. et al., 2016, *Comprehensive surface geophysical investigation of karst caves: A case study in the Xiaohayan section of the water supply project from Songhua River, Jilin*, Journal of Ap-

- plied Geophysics, Vol. 144, 37–49.
- BOCHYNEK M., 2016, *Karst caves of the Western Sudetes*, Poligrafia ad Rem, Jelenia Góra.
- BULLEN K.E., 1963, *An introduction to the theory of seismology*, Cambridge At The University Press.
- Detailed geological map of Poland on a scale 1:50 000 together with explanatory notes, sheet No. 796 Wojcieszów, Państwowy Instytut Geologiczny, Warszawa 2011.
- DZIEDZIC M., GRUSZECKI K., 1992, Geological Documentation of cambrian limestones Polom, kat C1, Arch. Przedsiębiorstwo Geologiczne we Wrocławiu, Proxima SA.
- HOEK E., BROWN E.T., 1980, *Empirical strength criterion for rock masses*, Jour. Geot. Engin. Div., 1013–1025.
- EN ISO 22476-3, 2005. *Geotechnical investigation and testing – Field testing. Part 3: Standard penetration test*.
- <https://jaskiniepolski.pgi.gov.pl/Details/Information/3986>
- KASPRZAK M., SOBCZYK A., KOSTKA S., HACZEK A., 2015, *Surface geophysical surveys and LiDAR DEM analysis combined with underground cave mapping – an efficient tool for karst system exploration: Jaskinia Niedźwiedzia case study (Sudetes, SW Poland)*. [In:] J. Jasiewicz, Z. Zwoliński, H. Mitasova, T. Hengl (red.), *Geomorphometry for Geosciences*, Adam Mickiewicz University in Poznan, International Society for Geomorphometry, Poznan, 75–78.
- KOTYRBA A., 2018, 3th Conference Construction of Civil Engineering Objects in Mining Areas. *Diagnosis and control of the sinkhole threat*, PZITB, Katowice, 1–14.
- KURPIEWSKI A., 2018, *Prognosis of the environmental impact of the findings of the draft amendment of the study of conditions and directions of spatial development of the town of Wojcieszów*, Zakład Ochrony Środowiska „Decybel”.
- NAZARIAN S., STOKOE II, K.H., HUDSON W.R., 1983, *Use of spectral analysis of surface waves method for determination of moduli and thicknesses of pavement systems*, Transportation Research Record, No. 930, 38–45.
- PARK C.B., MILLER R.D., XIA J. et al., 1997, *Multi-Channel Analysis of Surface Waves (MASW). A summary report of technical aspects, experimental results, and perspective*, Kansas Geological Survey, USA, Open-file Report#97-10, 2-26.
- PN-EN 1997-1, 2008. Eurocode 7. *Geotechnical design. Part 1: General principles*.
- PN-EN 1997-2, 2009. Eurocode 7. *Geotechnical design. Part 2: Reconnaissance and investigation of the ground*.
- SANCHEZ-SALINERO I., ROESSET J.M., SHAO K.Y., STOKOE II, K.H., and RIX G.J., 1987, *Analytical evaluation of variables affecting surface wave testing of pavements*, Transportation Research Record, No. 1136, 86–95.
- SANTAMARINA J.C., 1994, *An introduction to geotomography*. [In:] R.D. Woods (Ed.), *Geophysical characterization of sites*, ISSMFE Technical Committee #10, Oxford Publishers, New Delhi.
- SHEU J.C., STOKOE I.I., ROESET J.M., 1988, *Effect of reflected waves in SASW testing of pavements*, Tran. Res. Rec., No. 1196, 51–61.
- SOBCZYK A., KASPRZAK M., MARCISZA A., 2016, *Karst phenomena in metamorphic rocks of the Śnieżnik Massif (East Sudetes): state-of-the-art and significance for tracing a Late-Cenozoic evolution of the Sudetes*, Przegląd Geologiczny, 64, 710–718.
- SZYNKIEWICZ A., 2012, *Trial GPR surveys (RAMAC/GPR) in the area of the Bear Cave in Kletno*. [In:] W. Ciężkowski W. (red.), *Jaskinia Niedźwiedzia w Kletnie w 45-lecie odkrycia*, Wrocław–Kletno, 137–152.
- SZYNKIEWICZ A., ZYZAŃSKA H., ZYZAŃSKI H., 2001, *Unterirdische Welt des Bober – Katzbach Gebirge*, Wydawnictwo ARiP, Fakty, Żary.
- US Army Corps of Engineers, 1994, Engineering Manual EM 1110-2-2504, Table 3-1.
- WIŁUN Z., 2010, *Outline of geotechnics*, WKŁ, Warszawa.

- YILMAZ O., 1987, *Seismic data processing*, S.M. Doherty (Ed.), Invest. in Geophysics, No. 2, Soc. of Expl. Geophys.
- ZYZAŃSKA H., 2000, *Kryształowa Cave*. [In:] Grotolajza, nr 4, Żagań.
- ŻUK K. et al., 2011, *Environmental impact report for the planned development of the limestone mine on Mt. Połom in Wojcieszów*, extended in 2012 and supplemented in 2014 by BULiGL.